




AKADÉMIAI KIADÓ

# Results from the further development of CGI inversion on simulation and field data systems

ÁKOS GYULAI<sup>1</sup>, ENDRE TURAI<sup>1</sup>,  
MÁTYÁS KRISZTIÁN BARACZA<sup>2\*</sup> , ENDRE NÁDASI<sup>1</sup> and  
GEORGE DANKÓ<sup>3</sup>

Central European  
Geology

67 (2024) 1, 1–12

DOI:

[10.1556/24.2023.00131](https://doi.org/10.1556/24.2023.00131)

© 2023 The Author(s)

<sup>1</sup> Department of Geophysics, University of Miskolc, Miskolc, Hungary

<sup>2</sup> Research Institute of Applied Earth Sciences, University of Miskolc, Miskolc, Hungary

<sup>3</sup> University of Nevada, Reno, NV, United States of America

Received: July 27, 2023 • Accepted: December 23, 2023

Published online: March 25, 2024

## RESEARCH ARTICLE



### ABSTRACT

A new series expansion-based method, the Combined Geoelectric Weighted Inversion (CGWI) procedure is presented and tested by using synthetic and in-field measured datasets. The method is an improved version of the Combined Geoelectric Inversion (CGI) robustified by involving Cauchy-Steiner weights in an Iteratively Reweighted Least Squares technique. The new procedure is compared to the Fourier series expansion-based 1.5D and the CGI methods as well as to the broadly applied RES2DINV inversion procedure. The field measurements are performed during stone exploration in an active quarry on the south-western slopes of the Mátra mountains, in northern Hungary. It is shown that the CGWI method gives stable and robust parameter estimation with acceptable accuracy. The comparison with other inversion methods is based on data distances, estimation errors and correlation parameters calculated on the base of the parameter correlation matrix.

### KEYWORDS

geologic structures, geoelectric inversion, Wenner array, RES2DINV

## INTRODUCTION

Geoelectric measuring and evaluation systems are under intensive development today with the primary focus on shallow and medium-depth explorations. Geoelectric methods using multielectrode array systems, as well as traditional Vertical Electrode Sounding (VES) are all applied. Measured VES curves are usually evaluated by inversion at every station separately. The evaluation of data is traditionally performed by individual inversion applications developed a long time ago (Koefoed, 1979) and 1D approximation, which can hardly be applied for specifying complex geological structures in shallow depth with sufficient accuracy. Multielectrode measurements are applied more often to increase lateral resolution (Loke and Barker, 1996), using computer-controlled data collection from a multitude of electrodes, resulting in an efficient measuring technique. Inversion processing of the data is often performed by the RES2DINV software (Geotomo Software).

In order to achieve acceptable inversion results it is very important to find appropriate discretization, representing a reasonable balance between resolution and stability. In one hand there is a need to reach as high resolution as possible, this implies the use of large number of unknowns. On the other hand we have usually “inaccurate, insufficient and inconsistent” noisy data set (Jackson, 1972), which makes it possible to determine (uniquely and accurately) only a limited number of unknowns. This problem can be closely related to the forward modelling algorithm, used in the inversion procedure. At the first sight, it seems reasonable to use as accurate forward modelling method, as possible. In a lot of cases this requirement implies the

\*Corresponding author. Research Institute of Applied Earth Sciences, University of Miskolc, A/2. 1/4., 3515 Miskolc-Egyetemváros, Hungary. E-mail: [krisztian.baracza@uni-miskolc.hu](mailto:krisztian.baracza@uni-miskolc.hu)

use of FD or FEM procedures in calculating the theoretical data. The accurate calculation usually requires large number of grid points, or a dense mesh resulting in a large number of the unknowns (usually much higher than the number of measured data) in the inversion procedure. The use of a finer mesh for forward modelling and a coarser mesh for inversion (Cardarelli and Fischanger 2006), can help to find good compromise in handling the problem. It was noted by Sasaki (1989), that in the inversion of geoelectric data measured above 2D geological structures the solutions are frequently non-unique. As is well-known, there are various regularization and smoothing methods requiring additional assumptions in the model space. The constraints introduced to stabilize the solution are frequently out of geophysical meaning, having rather the mathematical nature of the solution is prescribed in them (minimum norm in the parameter space, smoothness operators etc.). On the other hand there are a lot of algorithms where it is possible to add physical inequality constraints that take into account geology, size and shape of anomaly (Cardarelli and Fishanger, 2006).

If we have no information in our (noisy) data set enough to determine all of these unknowns uniquely and accurately, the use of less accurate forward modelling procedures – containing only a limited number of unknown – can give a good compromise. This means, that inverting data sets, measured above a 3D geological structure, one can find more reliable results splitting the forward modelling procedure into a collection of 2D problems, and similarly, inverting data sets, measured above a 2D structure, one can find reliable results by splitting the forward modelling procedure into a collection of 1D problems.

Beard and Morgan (1991) demonstrated that 1D inversion can be a highly acceptable estimate in constructing contoured cross sections in case of some significant 2D subsurface structures. Auken et al. (2005) presented a piecewise 1-D laterally constrained inversion procedure for processing and interpreting very large data sets. The locally 1-D models are connected laterally by requiring approximate identity between neighbouring parameters within a specified variance (Auken and Christiansen, 2004). In our CGI approach, we propose an alternative way to reduce the non-uniqueness inherent in traditional 2-D inversion schemes. The essential part of the procedure is that we make the parameterization of a 2-D geoelectric earth model in terms of a series expansion of layer-thicknesses and resistivities and define the expansion coefficients as the unknowns of the inverse problem. This kind of parametrization ensures the lateral connection between neighbouring parameters (similarly as in Auken and Christiansen, 2004), on the other hand, it also gives the possibility to define the 2-D inversion problem as an overdetermined one, without the need for any additional regularization (or smoothness) constraint.

It was also demonstrated by Gyulai and Ormos (1999) that the investigation of 2D structures can efficiently be carried out by using local 1D forward modelling in the inversion of the DC geoelectric data measured in a set of arrays (parallel with the strike direction) equidistantly positioned along the dip direction of the geological structure. In their approach (called 1.5D

inversion) Fourier- as well as power series expansion were used in the discretization of the laterally varying thickness and resistivity functions of the 2D geological model. The authors proved, that with the appropriate choice of the number of independent unknowns (expansion coefficients) stable and accurate inversion algorithms can be defined. Series expansion-based inversion methods have been developed in details at the Department of Geophysics, University of Miskolc. Earlier a similar inversion algorithm was developed to solve the 2-D seismic guided-wave inverse problem by Dobróka et al. (1995) and a 2-D seismic refraction inverse problem by Bernabini et al. (1988) and by Ormos (2002) and Ormos and Daragó (2005), in which the lateral variation of the model was discretized by using series expansion and the inverse problem was formulated in terms of the expansion coefficients as unknowns. Further developments were presented by Cardarelli et al. (2014) in combining geoelectric and seismic datasets in a joint tomographic procedure. The integration of Electrical Resistivity Tomography and P- and SH-wave seismic measurements serve as a useful tool for imaging the geometry of the investigated earth body and characterizing the geoelectric and elastic properties. Further improvements were reached by integrating DC geoelectric and IP data in a large scale 2D or 3D joint inversion procedure (De Donno and Cardarelli, 2017).

As a part of the geoelectric methods and geoelectric inversion techniques, a grading method is developed based on the covariance matrix, which also considers the lateral changes in the evaluation. First, an original, 1.5D series expansion-based inversion method was developed (Gyulai and Ormos, 1997, 1999), followed by an improved variant using 2D series expansion-based geoelectric inversion, called CGI inversion (Gyulai et al., 2010, 2012, 2013). Further developments and tests followed, reported in the current work.

## METHOD DESCRIPTION

### Series expansion-based geoelectric inversion

The changes in the geometric (i.e. its layer boundaries) and physical (i.e. resistance) parameters of the geological structures can be expanded in series using an appropriately chosen set of basis functions. The unknown expansion coefficients can be determined in the framework of the inversion algorithm. In the knowledge of them, the (lateral and/or vertical) change of the geometric and physical parameters can be calculated.

In this paper, the Fourier series expansion is used to discretize the laterally changing model parameters as follows (Gyulai and Ormos, 1999):

$$\rho_n(s) = \frac{1}{2}d_{n_0} + \sum_{k=1}^{K_n} d_{nk} \cos k \frac{2\pi s}{s_p} + \sum_{k=1}^{K_n} d_{nk}^* \sin k \frac{2\pi s}{s_p}, \quad (1)$$

$$h_n(s) = \frac{1}{2}c_{n_0} + \sum_{l=1}^{L_n} c_{nl} \cos l \frac{2\pi s}{s_p} + \sum_{l=1}^{L_n} c_{nl}^* \sin l \frac{2\pi s}{s_p}, \quad (2)$$

where the  $n = 1, 2, \dots, N$  indexes are the number of layers ( $N$  is the total of the layers),  $\rho_n(s)$  is the resistivity function



of the  $n$ th layer,  $h_n(s)$  is the thickness function of the  $n$ th layer,  $s$  is the lateral coordinate along the profile,  $S_p$  is the length of the whole profile, while  $d_{nk}$ ,  $d_{nk}^*$ ,  $c_{nl}$ ,  $c_{nl}^*$  refer to the series expansion coefficients.  $K_n$  and  $L_n$  constants can be determined based on the VES stations.

### Combined geoelectric inversion (CGI)

The CGI inversion method was introduced by Gyulai et al. (2010). The CGI inversion algorithm contains two phases. In the first step, the model is estimated by a fast 1.5D inversion method (Gyulai and Ormos, 1999), which ensures an approximate solution after a few iteration steps. The 1.5D inversion demands only a very short CPU time, almost equivalent to that of the 1D inversion processes. In the linearized inversion algorithm, the least square method (LSQ) is applied for parameter identification. The covariance matrix utilized by Gyulai and Ormos (1999) was used to characterize the reliability and accuracy of the inversion process in the case of laterally slowly changing structures.

It provides the start model of the more time-demanding 2D inversion process in which the resistivity values in the grid cells are calculated using Eqs (1) and (2). The unknowns of the 2D inversion procedure are the expansion coefficients resulting in an overdetermined inversion giving higher stability and accuracy.

There are different coefficients used for characterizing the accuracy of the inversion results. During our investigations discussed in this paper, the data distance,  $d$ , the model distance,  $D$ , the estimation error (value of uncertainty),  $\sigma_{km}$ , the mean estimation error,  $F$ , and the mean spread,  $S$ , are determined.

In the data space the normalized data distance,  $d$ , is determined as follows:

$$d = \sqrt{\frac{1}{I} \sum_{i=1}^I \left( \frac{\rho_{a,i}^{(observed)} - \rho_{a,i}^{(calculated)}}{\rho_{a,i}^{(calculated)}} \right)^2} * 100\%, \quad (3)$$

where the  $I$  value of the formula represents the total number of the apparent resistivity data.

In the case of the inversion of synthetic data, it is important to calculate the relative model distance,  $D$ , as follows:

$$D = \sqrt{\frac{1}{M} \sum_{i=1}^M \left( \frac{m_i^{(estimated)} - m_i^{(exact)}}{m_i^{(exact)}} \right)^2} * 100\%, \quad (4)$$

where  $M$  is the total number of model parameters.

The accuracy of parameter estimation is often characterized by variances, which can be obtained from the diagonal elements of the covariance matrix after Menke (1984). For each VES station, the elements of the covariance matrix can be calculated. Since the covariance matrix is primarily calculated based on the series expansion coefficients ( $COV_{ij}$ ) of the inversion process, the covariance matrix of the layer parameters (calculated by using the law of error propagation) are used for evaluating the estimation error (value of uncertainty) as follows:

$$\sigma_{km} = \sigma_k(x_m) = \frac{\sqrt{\sum_{i=1}^{I(k)} \sum_{j=1}^{J(k)} \{ \Psi_{ki}(x_m) * \Psi_{kj}(x_m) * COV_{ij} \}}}{p_k(x_m)}, \quad (5)$$

where  $\sigma_k(x)$  represents the estimation error of the  $k$ -th model parameter (i.e. thickness or resistivity), while  $\sigma_{km}$  represents the same for the  $m$ -th VES station (at  $x = x_m$ ); the total value of the  $K$  number for the  $p_k(x)$  model parameters ( $k = 1, 2, \dots, K$ ) and  $M$  is the number of VES stations along the profile ( $m = 1, 2, \dots, M$ );  $J(k)$  is the number of basis functions of the  $k$ -th model parameter;

$\Psi_{ki}(x)$  and  $\Psi_{kj}(x)$  are the  $i$ -th and the  $j$ -th basis functions belonging to the  $k$ -th model parameter;  $COV_{ij}$  is the covariance matrix whose elements are calculated using the generalized inverse (Menke, 1984) given by the inversion procedure formulated for the expansion coefficients.

To give the general accuracy of the parameter estimation related to the whole model, the  $F$  mean estimation error (in percentage) is applied as follows:

$$F = \sqrt{\frac{1}{KM} \sum_{k=1}^K \sum_{m=1}^{M_k} \sigma_{km}^2} * 100(\%). \quad (6)$$

The Pearson correlation matrix is frequently used to characterize the degree of correlation between the estimated model parameters:

$$CORR_{ij} = \frac{COV_{ij}}{\sqrt{COV_{ii}COV_{jj}}}. \quad (7)$$

Due to the high number of the matrix elements, it is useful to introduce only one scalar parameter:

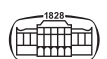
$$S = \sqrt{\frac{1}{P(P-1)} \sum_{j=1}^P \sum_{i=1}^P (CORR_{ij} - \delta_{ij})^2}, \quad (8)$$

which is called mean spread (Menke, 1984), as a general parameter describing the model correlation. In Eq. (8),  $P$  represents the total number of model parameters, while  $\delta_{ij}$  is the Kronecker-delta. The lower the value of  $D$ ,  $F$ , and  $S$  parameters of the whole inverted profile, the more reliable the 1.5D and CGI inversion results are.

In the inversion of field data, only  $d$ ,  $F$  and  $S$  can be used for the characterization of the inversion results. The  $D$  model distance can also be used for the investigations performed with synthetic data. The determination strategy of the optimal number of parameters ( $P$ ) is described by Gyulai et al. (2010). Using this strategy, the highest possible number of series expansion coefficients (i.e. the most complicated geological model) is accepted as the solution of the inverse problem, where values of the  $d$  data distance are determined from the measured and calculated data and the  $F$  mean estimation error are minimal at the same time.

### Combined geoelectric weighted inversion (CGWI)

In the geoelectric practice, it often occurs that various elements of the data sets are contaminated by appreciably different measurement errors Gyulai et al. (2014). Drahos



and Drahos et al. (2008, 2011) published a joint inversion method for processing with Gaussian distribution data, where the key factor of the strategy is automatic weighting. The combined geoelectric weighted inversion method (CGWI) also applies a special, automatic weighting for the evaluation of the measured data as shown in Fig. 1.

As shown in Fig. 1, the first step of the CGWI is a 1.5D inversion, followed by iterative cycles of weighted CGI inversions. At the end of the process, when the method reaches the defined stop criterion, the procedure gives the geoelectric model characteristics. The reliability evaluation of the inversion results is implemented in the process, using the qualification parameters introduced above.

Complex geological structures with many unknown factors are usually investigated by using inversion procedures. The number of unknown factors is typically large, often exceeding the number of measured data, resulting in an underdetermined problem. In our CGWI approach, the Fourier series expansion method allows reducing the number of unknowns (expansion coefficients), resulting in an overdetermined inverse problem that can be solved with a least-square (LSQ) fitting method for higher accuracy and stability. The algorithm developed by the authors focuses on decreasing the number of unknown factors in order to approximate complex (even 3D) structures.

The main concept in reducing the number of unknown parameters is to approximate the 3D formations with elongated, lower-dimensional structures, overlaid in different directions. With this effort, the real structure can be approximated better and faster. The measuring area is

often covered by profiles however, it is not known how the profiles are aligned with the dip or strike directions of a given geologic structure. Using a special (Steiner) weighting, the method iteratively selects the data which best match the elongated structure with the least LSQ fitting error.

The operating strategy of the inversion algorithm is shown in Fig. 2. Using this novel strategy, the CGWI method provides reliable inversion results for complex geological structures. The numerical method automatically evaluates the reliability parameters of the inversion results. These parameters may vary along the profiles and the user can decide to accept or refine the inversion by adding more VES stations for improved model fit.

The method assumes that the geological structure can change in both directions, i.e. the VES stations along the profile or the geoelectric data of the same VES station can be similar to both the dip or strike direction geological structures. As shown in Fig. 2, there are two types of elongated geological structures along the different geoelectric profiles. However, before the measurement, it is not known which data belong to dip or strike directions and which are the main directions of the geological structure.

Based on field experiences, it is useful to presume the appearance of both data types along the same profile. Steiner's Most Frequent Value (MFV) method takes into account the difference from the 2D structure by the automatic weighting of the data (Steiner, 1988, 1991, 1997), a useful process for the separation of measured data and the determination of the structure with a combined inversion technique available (Gyulai et al., 2017).

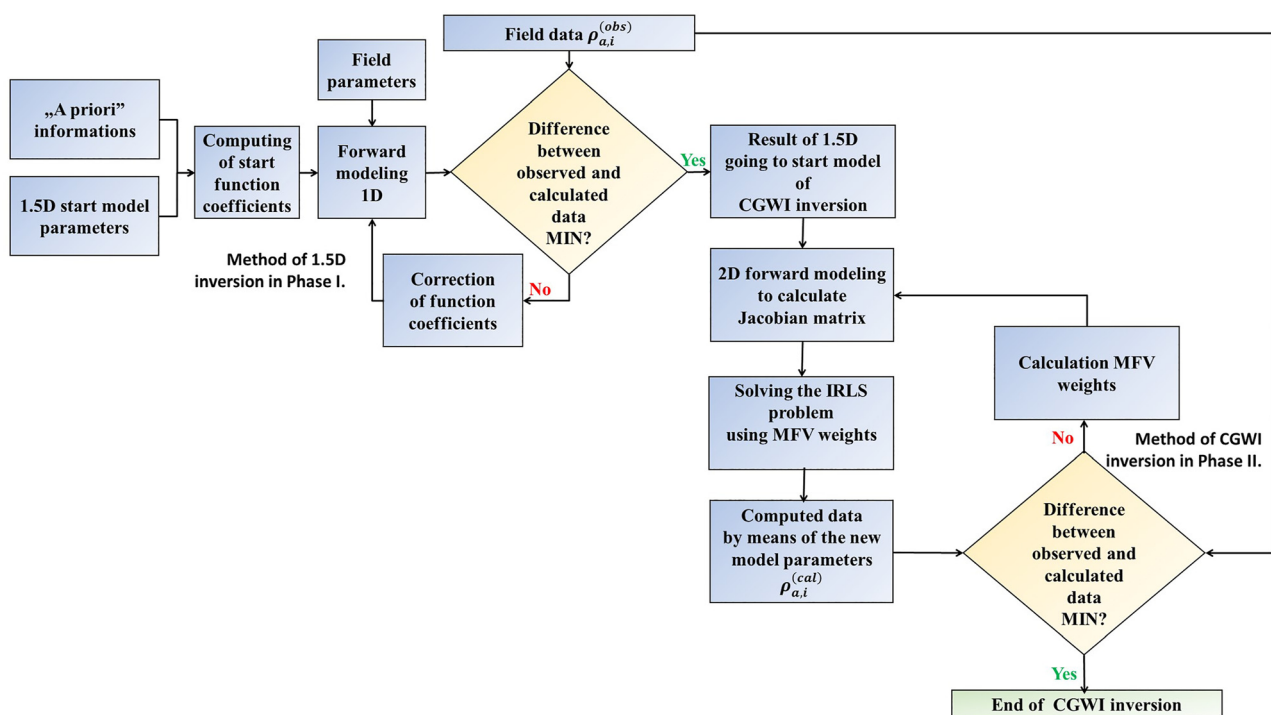


Fig. 1. Flow chart of CGWI inversion



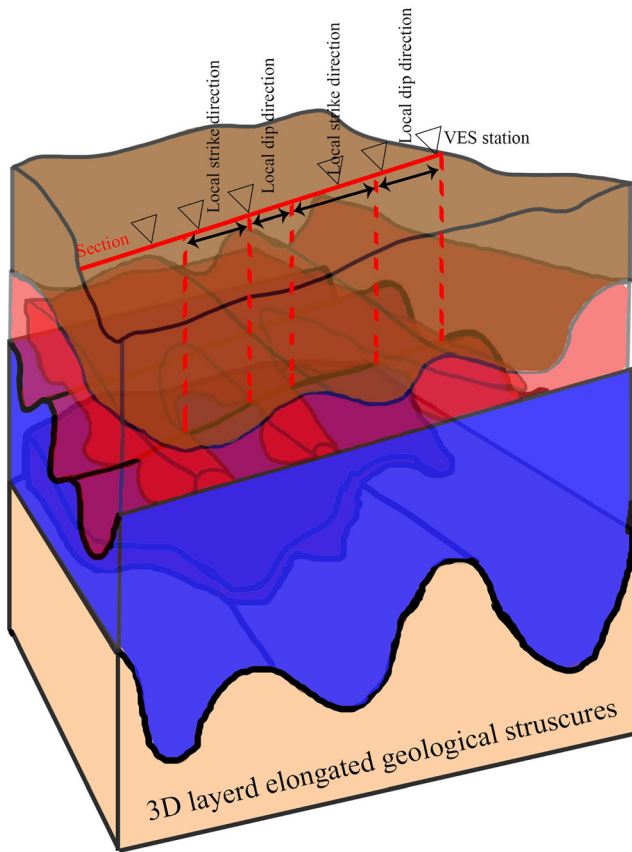


Fig. 2. Realization of CGWI inversion over different geological structures

The diagonal weight matrix should be recalculated in each iteration by application of the most frequent value (MFV) method:

$$W_{ij} = \begin{cases} \left( \frac{\varepsilon_{l+1}^2}{\varepsilon_{l+1}^2 + y_j^2} \right) & \text{if } i = j \\ 0 & \text{otherwise} \end{cases}, \quad (9)$$

where  $y_j$  is the  $j$ -th residual and the dihesion:

$$\varepsilon_{l+1}^2 = 3 \frac{\sum_{j=1}^N \frac{y_j^2}{\varepsilon_l^2 + y_j^2}}{\sum_{j=1}^N \frac{1}{\varepsilon_l^2} - y_j^2}, \quad (10)$$

where the  $\varepsilon_l^2$  values can be obtained from the value estimated from the previous iteration step (Steiner, 1988). The initial  $\varepsilon_0$  value can be chosen as:

$$\varepsilon_0 \leq \frac{\sqrt{3}}{2} (y_{max} - y_{min}) \quad (11)$$

By using Steiner's method, the data with high residual get only minimal weight in the inversion result. The MFV procedure gives reduced weights when the residual is high independently of its reason: the presence of outlying measurement error or the occurrence of large model error (for example the strike forward modeling formula is applied for data collected along a direction near to the dip, or vice versa).

The inversion algorithm makes a forward model on the input data using sets of dip and strike direction readings, from which, as a result of Steiner's weighting method, the algorithm separates them into dip-like and strike-like data. Thus, during the CGWI inversion process, the selected types are separated simultaneously. Determination of the spatial distribution of layer parameters needs further interpolation. Combined inversion of different direction data sets along the same profile makes the realization of the 3D interpretation available with adequate accuracy. As the information matrixes of the data sets measured in multi-direction profiles can differ from each other, this connection can rather be referred to as a joint inversion procedure. The availability of the noise rejection effect of robust MFV method introduced by Dobróka et al. (2016).

Substituting Steiner's weights into the equation of the inversion method, the following formula can be written (Menke, 1984):

$$G^T W G p = G^T W \rho \quad (12)$$

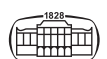
where  $G$  is the Jacobi matrix,  $W$  is the weight matrix,  $p$  is the (unknown) model vector and  $\rho$  is the vector of the measured (input) data.

As a consequence, the high residuals influence the result of the estimation only to a relatively small extent (Using the MFV weights the normal equation (9) become nonlinear, so to solve it the Iteratively Reweighted Least Squares method developed by Scales et al. (1988) should be utilized.). In addition, Steiner's method of weights used in the CGWI inversion method allows the evaluation of the slowly changing 3D geological structures as well.

## INVERSION INVESTIGATIONS USING SYNTHETIC DATA

The methods described in the foregoing are tested against synthetic data for performance evaluation. The first investigation is a test of CGI inversion using a known geologic structure with synthetic data from a computational model. The input data came from only one section, but Steiner's weights are still applied in the inversion. The input data are calculated without adding error noise, using a 3D forward modeling technique (Spitzer, 1995) on a complex, 2D-3D model combination. In the 2D inversion, the appearance of data and estimation error is expected because of the 2D model approximation. The aim of investigation tests on synthetic data is to assess the goodness of fit of inversion results. To perform this, comparative investigations are provided.

Figure 3a-d presents the results of the inversion for a single section of the model. Figure 3a shows dip directional inversion result that is the most important information in geoelectrical practice. The mean estimation error obtained for parameter determination is 30%. The inversion utilizes 352 pieces from 493 data, which means 71% of all data are represented according to the rule of Steiner weighting.



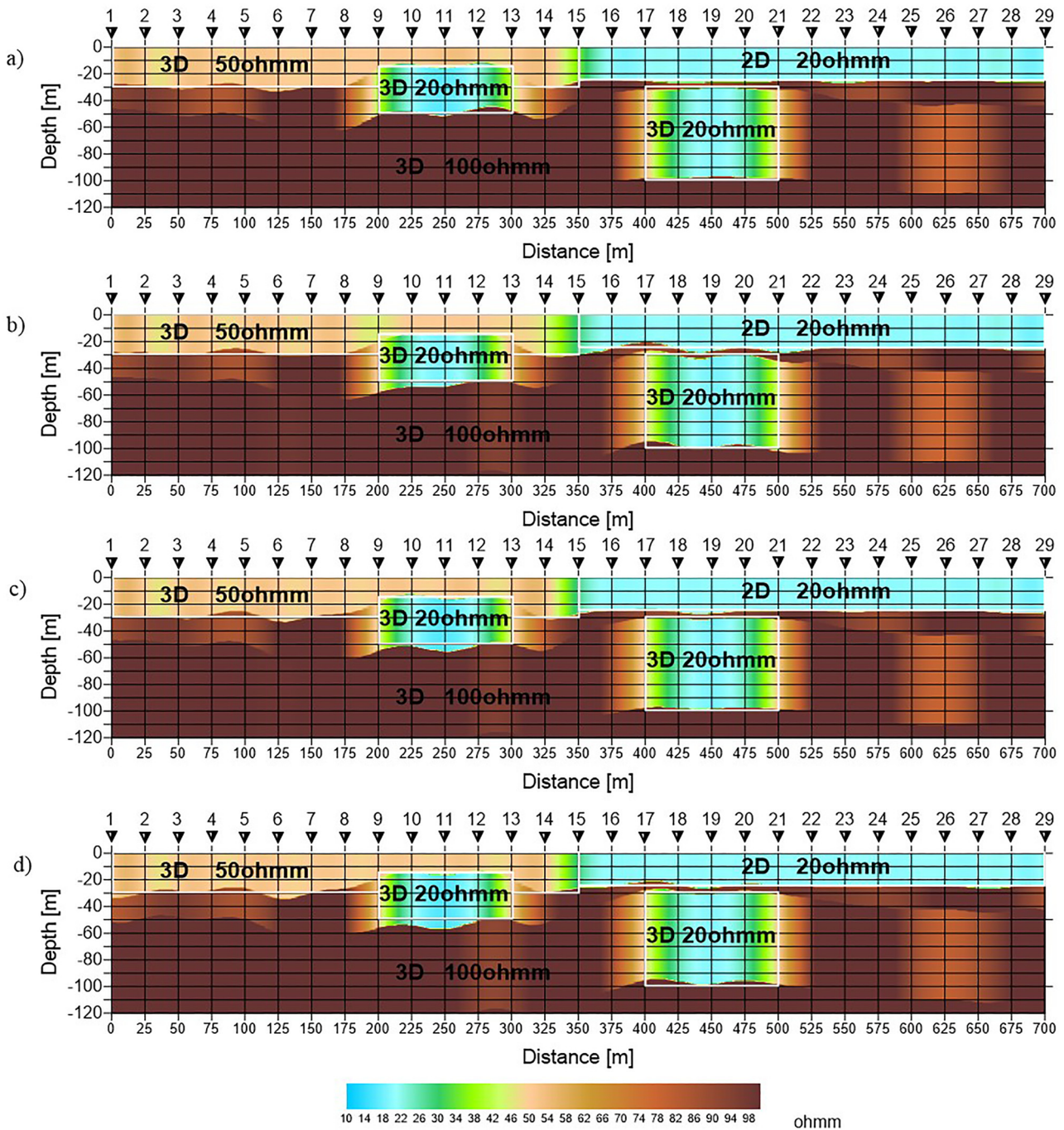


Fig. 3. Result of CGI and CGWI

a) dip directional Fourier series expansion-based inversion, on dip directional synthetic data set, b) dip directional Fourier series expansion-based inversion, on strike directional synthetic data set, c) dip directional Fourier series expansion-based inversion, on strike and dip directional synthetic data set, d) series expansion-based inversion, on strike and dip directional synthetic data set

Figure 3b shows the case when the specific direction of the structure is unknown. It means that our data set originate from strike directional synthetic data, but they are attached to the inversion as dip directional data. In this case, the mean error of the estimation is 114% for the inversion that utilizes only 188 pieces of data.

Assuming the wrong directions for the dip and strike in the structure may cause a large inversion error, originating

from two components. Firstly, a forward modeling algorithm is used in CGI inversion for dip directional synthetic data. Secondly, the information content of strike directional data can be quite different from the dip directional ones.

In the case of one single section, the problem of mixing the dip and strike directional data must be addressed. To investigate this problem, a data system that contains dip and strike directional data together must be chosen, so the

specific direction of the geological structure is changing inside the section. Figure 3c shows the CGI dip directional inversion result for this kind of mixed data system. It is assumed in the inversion that every data is measured in a dip direction. The mean estimation error for this case becomes 55% while the inversion utilizes only 281 pieces of data from 493 in this case. The estimation error and the utilization are between the values of 30% and 114% of the previous two cases as shown in Table 1, but associated with Fig. 3a and c.

Figure 3d shows the result of CGWI inversion for a mixed data set. Since it is unknown which data belong to strike and which to dip direction, it is assumed that the data system is dip directional in one section and strike directional in the other section. It is acknowledged that both sections contain data that do not fit in their section based on the assumption. That is, in the inversion, the doubled data system is jointly involved but as measurements with different directions (synthetic data) with respect to the structure. This gives a total of 986 data. It is important to understand that this is not simply a replication of data. Of the 986 data, the actual "measured" data is only 493. Automatic sorting of the data is performed by Steiner weighting within the CGWI inversion. The results presented in Fig. 3d show a mean estimation error of 23%, which is much less than 55% in the previous case as shown in Table 1, but associated with Fig. 3c. The inversion utilized 415 pieces of data from joint data system with automatically applying the Steiner filters. It is also interesting to note that, the result is better than that in case of dip directional inversion of dip directional data (Fig. 3a), where the mean estimation error was 30% as has presented in Table 1. Inversion quality parameters for the figures containing synthetic data Fig. 3a-d are summarised in Table 1.

As it can be seen, in CGWI inversion the *D*, *F* and *S* characteristics show sufficient improvements compared to the previous methods. At the same time this improvement results in higher stability and estimation accuracy of the CGWI inversion procedure. Due to these advantages the use of CGWI can be suggested in spite of its higher computation time requirement.

The results in Fig. 3d show that, although we did not apply any additional "measurement" (in this case synthetic) data to the inversion and did not make any assumptions on the directions of the structure, we only "gave the option" to

the inversion to choose/mark on its own which data represent dip directional data and which data represent strike directional data, based on the algorithm we developed. These synthetic model studies provide convincing evidence that the use of CGWI inversion can significantly improve the accuracy of the evaluation and at the same time increase the resolution of the research. By improving both aspects, we can obtain much more detailed and reliable results in geological and hydrogeological research.

As shown, the CGWI algorithm performs at a higher accuracy of evaluation on synthetic data than the other applied methods. This means also a higher resolution of the exploration of the geologic structure.

## INVERSION INVESTIGATIONS IN FIELD CASES

Two methods are chosen to compare the results and to solve the inverse problem: the series expansion-based inversion developed by the authors and the tomographic method based on the RES2DINV inversion program.

The pre-Cenozoic basement of the area is composed of Neopalaeozoic and Mesozoic formations have undergone very little metamorphism.

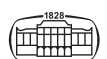
The stratigraphic position of the Nagyhársasi Andesite Formation is Lower- Badenian. It is deposited onto the Tari Tuff and is overlain by the Szurdokpüspöki Diatomite- also of Badenian-, the Gyöngyösolymos Riolite and the Kékesi Andesite Formations.

Regarding the lithogenesis, it has stratovolcanic structure. It is formed by the stacking of several eruptive centres and formed the so called „middle andesite of the Mátra Mountains". Lithologically it is composed of pyroxene andesite lava, agglomerate, tuff, and in some places interbedded riolite and dacite tuff. On the south and east The Nagyhársas Andesite Formation is bounded by proluvial and slope movement sediments (Gyalog and Budai, 2004).

As this is a volcanic area, where andesite, tuff, weathered andesite tuff and clay deposits from their decomposition alternate, the variability and distribution of the rocks is high. The resistivity of andesites reaches around 200 ohmm, while that of clays is barely around 1-2 ohmm, which probably contain large amounts of bound water.

Table 1. Information on the inversion evaluations using synthetic models and a summary table of the parameters that qualify the results

	Qualifying parameters the inversion results			Effective number of data			Nb. of expansion coefficients	
	Model distance (D)	Mean estimation error (F [%])	Mean spread (S)	Utilized data number of inversion	Total number of data	Utilized data number in percentage [%]	Layer thicknesses	Resistivities
Figure 3a	0.67	30	0.179	352	493	71	25 – 9 – 1	29 – 13 – 11 – 1
Figure 3b	0.7	114	0.26	188	493	38		
Figure 3c	0.8	55	0.186	281	493	56		
Figure 3d	0.4	23	0.176	415	986	42		



## EVALUATION OF FIELD MEASUREMENTS WITH THE SERIES EXPANSION BASED INVERSION

Comparing the two methods, the data of two 110 m long apparent resistivity (pseudo-)sections are used, which are measured with 5 m electrode spacing in the Wenner array. The 110 m long section is only a part of the whole profile, chosen randomly for comparing the methods.

In addition to keeping the color scales the same in the figures, densely spaced isocurves are also shown for the apparent resistivities to aid the comparison. As shown in Fig. 4, the CGWI inversion better highlights the values of resistivity parameters, when compared to the measured, apparent resistivity values. The reference depths of the apparent resistivities are also plotted on two different scales. In one case it was  $AB/2m$ , in the other  $AB/4m$ . In our experience, for 2D (quasi 3D) structures, the latter is closer to the depth structure of the inverted section.

The visualization predicts the expected result of inversion for the contours of the geologic structure. Staying in the data space, Fig. 5 shows the filtered version of *with vertical depth* ( $AB/2$  and  $AB/4$ ) in Fig. 4.

It can be noticed that bold isocurves indicate the layer boundaries quite well: the blue lines are for the lower resistivities, while the red lines with the warm-coloured fills indicate the direction of the transition to the higher resistivities. This type of visualisation can help to identify trends in the measured data immediately after the field measurement is completed. This simple solution seems to be

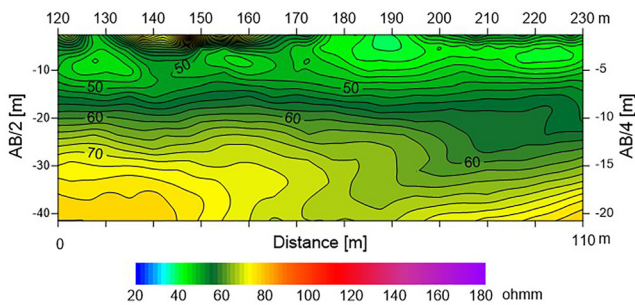


Fig. 4. Pseudo section in Apc 2 profile with vertical depth ( $AB/2$  and  $AB/4$ )

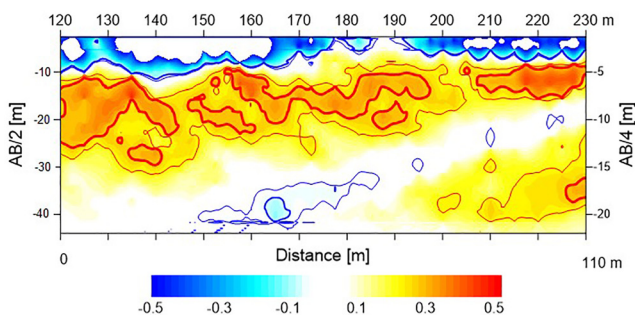


Fig. 5. Filtered pseudo section of Fig. 4 (shift and difference filter in Surfer 8 software)

advantageous for describing the geometric characteristics of the structure.

Figure 6a–d shows the results of the inversion evaluations of the Apc 2 section on the DC geoelectric data system. The results of the 1.5D, CGI and CGWI inversion evaluations are shown in order in Fig. 6a–c. The results of the evaluation using RES2DINV software are shown in Fig. 6d. The data qualifying the results of the four different inversions shown in Fig. 6a–d and other relevant information are presented in Table 2.

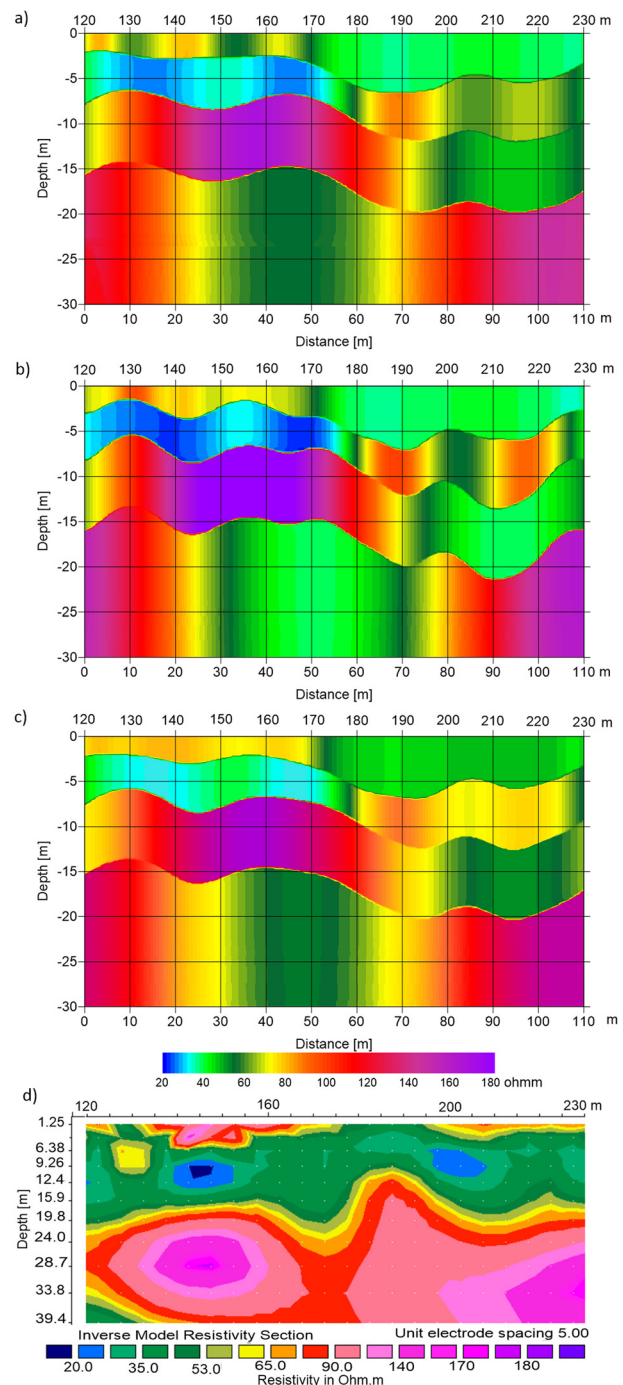


Fig. 6. Apc 2 field section results using a) 1.5D, b) CGI, c) CGWI, d) RES2DINV inversion techniques





Table 2. Summary table of the inversion parameters of the Apc 2 section and the qualifying values of the results

	RMS error [%]	Qualifying parameters of data			Nb. of expansion coefficients	
		Data distance (d)	Mean estimation error (F [%])	Mean spread (S)	Layer thicknesses	Resistivities
Figure 6a	–	2.1	65	0.304	17 – 11 – 1	23 – 9 – 3 – 3
Figure 6b	–	2.5	94	0.262		
Figure 6c	–	2	37	0.222		
Figure 6d	1.2	–	–	–	–	–

On one hand, the essence of the improvement is the application of the MFV approach to properly control the contribution of each data in the solution of the inverse problem. This weighting process is fully automated and does not require preliminary knowledge of the data distribution. The sensitivity of inversion to data noises especially outliers can be highly reduced by using this robust statistical method. On the other hand, to achieve good spatial resolution, we also automatically optimize the number of coefficients in the series expansion-based inversion process so that the data distance and the mean estimation error for the estimated resistivities have their minimum value simultaneously.

In relation to Figs 6a–c and 9a–c, we would like to note that the undulating character shown in the figures is due to the fact that we have worked with relatively lower numbers of expansion coefficients in the Fourier series expansion in order to achieve greater stability of the procedure. The undulating feature can be reduced by increasing the number of the expansion coefficients with the consequence of less stable inversion procedure.

The data system of section 2 using the Apc 2 profile is evaluated based on the inversion algorithm of Loke and Barker (1996), using the RES2DINV software (Geotomo, RES2DINV 3.55). The data is collected in a Wenner array with 5 m electrode distances. The resistivity image made by the RES2DINV inversion is presented in Fig. 6d. In Fig. 6d, the vertical axis represents the true depth and the horizontal axis represents the distance in metres along the section. The RMS difference between the results from the model and the measured apparent resistivity distribution is 1.2%. The color scale in Fig. 6d and that in Fig. 6a–c are the same for easy comparability. As shown in the figures, a poor conductor basement – at least 50 ohmm – can be seen under the depth of 15 m in both evaluations. The resistivity of the basement is decreased to about 75 ohmm in the middle of the section in Fig. 6d, while this value is slightly lower (50 ohmm) shown in Fig. 6a–c.

In the following, the results of the evaluation of the Apc 3 section are presented. The system of presenting the results is the same as in the section presented earlier. It is also important to note that similar remarks can be made in Apc 3 to those made in Apc 2 presented earlier.

The apparent resistivity values in Fig. 7 show the pseudo distribution profile of Apc 3.

In this section, too, it can be seen from the pseudo values that the structure of the strata is highly inhomogeneous and lacks the presence of high-resistance blocks typical of good

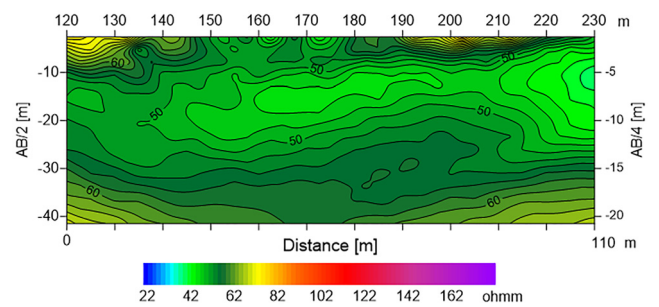


Fig. 7. The pseudo section in Apc 3 profile with vertical depth (AB/2 and AB/4)

quality rocks. To obtain better quality rock, it is necessary to remove significant thicknesses of covering layers. Unfortunately, even the lower part of the pseudo section does not show a uniform block that can be mined. In the upper 10–15 m, no usable rock is visible in terms of quality raw materials.

Figure 8 shows the filtered results of the pseudo section in Fig. 7 using the Surfer 8 software.

The filtered pseudo-section used to evaluate the Apc 3 section data also shows where the zones of lower resistivity rock layers change towards higher values, and where the good quality rocks change towards more degraded ones. This achieves the suggestion that this simple screening procedure is also useful for the interpretation of pseudo sections.

The inversion of the Apc 3 section with series expansion-based method required more variability (more coefficients) for the specific resistivity. Gyulai et al. (2010) developed a strategy to determine the number of coefficients for the application of the series expansion-based inversion. The idea is to use a coefficient number for which both the data

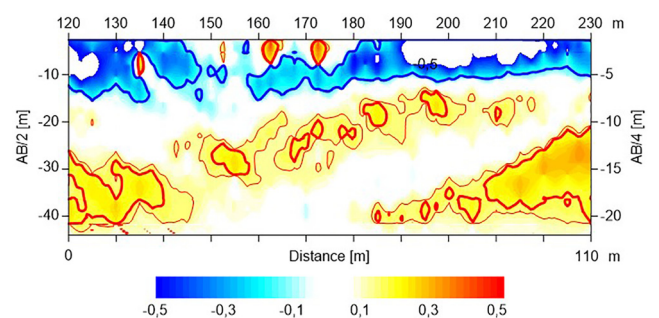
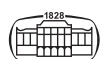


Fig. 8. Filtered pseudo section of Fig. 7 (shift and difference filter in Surfer 8 software)



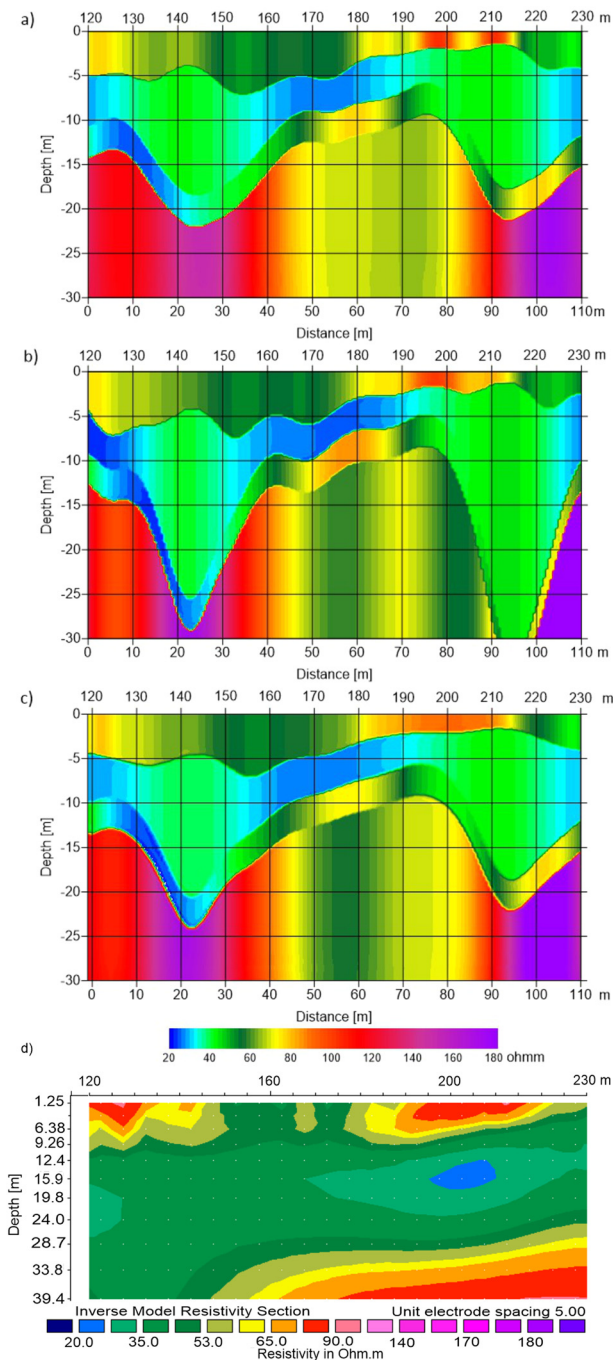


Fig. 9. Apc 3 field section results using a) 1.5D, b) CGI, c) CGWI, d) RES2DINV inversion techniques

distance and the mean error of the estimate are minimum. Figure 9a–d shows the results of the inversions of the Apc 3 section. The inversion results for 1.5D, CGI and CGWI are shown in Fig. 9a–c respectively. The results of the evaluation using RES2DINV software are shown in Fig. 6d. The data qualifying the results of the four different inversions shown in 6a–d and other relevant information are presented in Table 2.

In section 3, the CGI inversion shows significant uncertainty at 25 and 95 m. This may have increased the mean error of the estimation. It can be concluded that the mean estimation error of 37 (%) for Fig. 6c (Table 2), which shows the CGWI solution of section Apc 2, and the mean estimation error of 43 (%) for Fig. 9c (Table 3), which also shows the CGWI inversion results of section Apc 3, seem high at first impression, but a very significant part of them is due to the lack of measured data with shallow penetration. The data qualifying the results of the four different inversions shown in Fig. 9a–d and other relevant information are presented in Table 3.

The inversion evaluation with Geotomo software of multielectrode measurement using the Apc 3 section is shown in Fig. 9d, where the RMS deviation is 2.2% (value included in Table 3). Shown in Fig. 9d the vertical axis is the true depth and the horizontal axis is the distance in metres along the section. The poor conductor basement appears in a deeper position, and the dynamics of the change of resistivity and geometrical parameters is significantly lower than in the case of Fig. 9b and c.

### DISCUSSION AND CONCLUSIONS

Using Steiner’s weights the Combined Geoelectric Inversion method (CGI) is improved and the Combined Geoelectric Weighted Inversion procedure (CGWI) is developed. It is shown that the new method has two main advantages.

In solving 2-D or 3-D inversion problems with the FD forward modeling method piecewise constant resistivities defined on a rectangular grid of cells are assumed. This results in a large number of unknowns normally leading to an underdetermined inverse problem. To find a unique solution various additional (usually non-physical) constraints have to be applied. In the framework of the CGWI, the physical and geometrical model parameters are expressed in terms of a series expansion utilizing a suitably chosen system of basis

Table 3. Summary table of the inversion parameters of the Apc 3 section and the qualifying values of the results

RMS error [%]	Qualifying parameters of data			Nb. of expansion coefficients	
	Data distance (d)	Mean estimation error (F [%])	Mean spread (S)	Layer thicknesses	Resistivities
Figure 9a	2	71	0.31	17 – 11 – 1	23 – 9 – 7 – 9
Figure 9b	2.8	136	0.26		
Figure 9c	2.1	43	0.232		
Figure 9d	2.2	–	–	–	–



functions. This gives the possibility to sufficiently reduce the number of the expansion terms defining overdetermined inverse problems for the unknown expansion coefficients in 2D or even 3D cases.

The application of Steiner's weights reduces the contribution to the inversion results of the data with large residuals regardless of the reason for the increase (measurement or modelling error). This has the advantage of a good nose rejection if the measured data contains a sufficient portion of outliers. On the other hand in a field example, it is usually unknown which data belong to the strike and which to dip direction. In forward modelling, it is assumed that the data system is dip directional in one section and strike directional in the other section. In case of false assumption (dip data are forward modelled as strike ones or vice versa), large residuals occur resulting in low weights, consequently a reduced contribution to the inversion results. So an automatic sorting of the data is performed by Steiner weighting within the CGWI inversion.

The direct current geoelectric methods can be efficiently applied for mapping the geologic structure's boundaries for geological, hydrogeological, mining and environmental applications. Besides the classic VES methods, the multielectrode systems are getting more and more important in data collection. The efficiency of the 1.5D, CGI, and CGWI methods are compared to the RES2DINV program in two examples using synthetic as well as field data.

The overdetermined nature of the CGWI method results in stable and accurate parameter estimation. This is shown in numeric and in-field examples. It is found that on synthetic data, the CGWI series expansion-based geoelectric inversion provides better evaluation results for complex geologic structures which contain dip and strike direction structures than using the dip direction inversion of the CGI method of customary practice.

It is shown that the application of Steiner's automatic weighting method is advantageous in combination with the CGWI algorithm for highlighting or neglecting some data, depending on how much they are prominent compared to the adjacent data. With the application of this combined method, the accuracy of the evaluation and the resolution can be significantly improved. The quality criterion parameters based on the covariance matrix provide good information regarding the reliability of the parameter estimation.

The applicability of the CGWI inversion method is demonstrated in scaled figures, showing the evaluation results of the field data with favorable comparison to the results from the commercially available RES2DINV program for complex 2D and 3D geological situations.

It is demonstrated that the geoelectric series expansion-based inversion methods, and especially CGWI, can be applied efficiently and with an automatic quality check for geophysical exploration purposes.

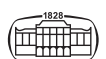
## ACKNOWLEDGEMENTS

The research was carried out in the framework of the GINOP-2.3.2-15-2016-00010 "Development of enhanced

engineering methods with the aim at utilization of subterranean energy resources" project of the Research Institute of Applied Earth Sciences of the University of Miskolc in the framework of the Széchenyi 2020 Plan, funded by the European Union, co-financed by the European Structural and Investment Funds.

## REFERENCES

- Auken, E. and Christiansen, A.V. (2004). Layered and laterally constrained 2D inversion of resistivity data. *Geophysics*, 69: 752–761.
- Auken, E., Christiansen, A.V., Jacobsen, B.H., Foged, N., and Sorensen, K.I. (2005). Piecewise 1D laterally constrained inversion of resistivity data. *Geophysical Prospecting*, 53: 497–507.
- Beard, L.P. and Morgan, F.D. (1991). Assessment of 2-D resistivity structures using 1-D inversion. *Geophysics*, 56(6): 874–883. <https://doi.org/10.1190/1.1443106>.
- Bernabini, M., Brizzolari, E., and Cardarelli, E. (1988). Interpretazione interattiva automatica di prospezioni sismiche a rifrazione. (Interactive automatic interpretation of refraction seismic investigation, in Italian) Atti del 7o Convegno Annuale del Gruppo Nazionale di Geofisica Della Terra Solida. *Roma* 11.30–12.02: 657–670.
- Cardarelli, E. and Fischanger, F. (2006). 2D data modelling by electrical resistivity tomography for complex subsurface geology. *Geophysical Prospecting*, 54: 121–133.
- Cardarelli, E., Cercato, M., and De Donno, G. (2014). Characterization of an earth-filled dam through the combined use of electrical resistivity tomography, P- and SH-wave seismic tomography and surface wave data. *Journal of Applied Geophysics*, 106: 87–95.
- Dobróka, M., Fancsik, T., and Amran, A. (1995). On the in-seam seismic inverse problem. *57th EAEG Meeting*, Glasgow, 29 May–2 June.
- Dobróka, M., Szabó, N.P., Tóth, J., and Vass, P. (2016). Interval inversion approach for an improved interpretation of well logs. *Geophysics*, 81(2): D163–D175.
- De Donno, G. and Ettore Cardarelli, E. (2017). VEMI: a flexible interface for 3D tomographic inversion of time- and frequency-domain electrical data in EIDORS. *Near Surface Geophysics*, 15: 43–58.
- Drahos, D. (2008). Determining the objective function for geophysical joint inversion. *Geophys Transactions*, 45: 105–121.
- Drahos, D., Gyulai, Á., Ormos, T., and Dobróka, M. (2011). Automated weighting joint inversion of geoelectric data over a two dimensional geologic structure. *Acta Geod. Geophys. Hung.*, 46: 309–316.
- Geotomo software: RES2DINV ver.3.55, Malaysia [www.geoelectrical.com](http://www.geoelectrical.com).
- Gyalog, L. and Budai, T. (2004). *A Magyar Állami Földtani Intézet Évi Jelentése, 2002 (2004), Javaslatok Magyarország földtani képződményeinek litosztratigráfiai tagolására*. Proposal for new lithostratigraphic units of Hungary, Budapest, p. 220.
- Gyulai, Á. and Ormos, T. (1997). Interpretation of vertical electrical sounding curves with 1.5-D inversion method (in Hungarian) *Magyar Geofizika*, 38(1): 25–29.



- Gyulai, Á. and Ormos, T. (1999). A new procedure for the interpretation of VES data: 1.5-D simultaneous inversion method. *Journal of Applied Geophysics*, 41: 1–17.
- Gyulai, Á., Ormos, T., and Dobróka, M. (2010). A quick 2-D geoelectric inversion method using series expansion. *Journal of Applied Geophysics*, 72: pp232–241.
- Gyulai, Á., Turai, E., and Baracza, M.K. (2012). The analysis of CGWI inversion results involving a field case (in Hungarian). *Magyar Geofizika*, 53(4): 267–274.
- Gyulai, Á., Baracza, M.K., and Tolnai, É.E. (2013). The application of joint inversion in geophysical exploration. *International Journal of Geoscience*, 4: 283–299.
- Gyulai, Á., Baracza, M.K., and Szabó, N.P. (2014). On the application of combined geoelectric weighted inversion in environmental exploration. *Environmental Earth Sciences*, 71: 383–392.
- Gyulai, Á., Szűcs, P., Turai, E., Baracza, M.K., and Fejes, Z. (2017). Geoelectric characterization of thermal water aquifers using 2.5D inversion of VES measurements. *Surveys in Geophysics*, 38: 503–526.
- Jackson, D.D. (1972). Interpretation of inaccurate, insufficient and inconsistent data. *Geophysical Journal*, 28(2): 97–109. <https://doi.org/10.1111/j.1365-246X.1972.tb06115.x>.
- Koefoed, O. (1979). *Geosounding principles 1: resistivity sounding measurements*. Elsevier, Amsterdam.
- Loke, M.H. and Barker, R.D. (1996). Rapid least-square inversion of apparent resistivity pseudo-sections by a quasi-Newton method. *Geophysical Prospecting*, 44: 131–152.
- Menke, W. (1984). *Geophysical data analysis-discrete inverse theory*. Academic Press, Inc., London.
- Ormos, T. (2002). Inversion of refracted travel-times for near-surface investigations. *EAGE 64th Conference and Exhibition*, 27–30 May. 2002. Florence, Italy. D025 Extended abstracts.
- Ormos, T. and Daragó, A. (2005). Parallel inversion of refracted travel times of P and SH waves using a function approximation. *Acta Geodaetica and Geophysica Hungarica*, 40: 215–228.
- Sasaki, Y. (1989). Sensitivity analysis of magnetotelluric measurements in relation to static effects. *Geophysical Prospecting*, 37(4): 395–406. <https://doi.org/10.1111/j.1365-2478.1989.tb02213.x>.
- Scales, J.A., Gersztenkorn, A., and Treitel, S. (1988). Fast Lp solution of large, sparse, linear systems: application to seismic travel time tomography. *Journal of Computational Physics*, 75: 314–333.
- Spitzer, K. (1995). 3D finite difference algorithm for DC resistivity modelling using conjugate gradient methods. *Geophysical Journal International*, 123: 902–914.
- Steiner, F. (1988). Most Frequent value procedure (A short monograph). *Geophysical Transactions*, 34: 139–260.
- Steiner, F. (1991). *The most frequent value. Introduction to a modern conception of statistics*. Academic Press, Budapest, ISBN 9630556871.
- Steiner, F. (1997). *Optimum methods in statistics (English)*. Akadémiai Kiadó, Budapest, ISBN 963057439X.

